# Modeling Environmental Effects on Directionality in Wireless Networks

Eric Anderson, Caleb Phillips, Dirk Grunwald, and Douglas Sicker

CU-CS-1044-08 July 2008

University of Colorado at Boulder

Technical Report CU-CS-1044-08
Department of Computer Science
Campus Box 430
University of Colorado
Boulder, Colorado 80309

# Modeling Environmental Effects on Directionality in Wireless Networks

Eric Anderson, Caleb Phillips, Dirk Grunwald, and Douglas Sicker

July 2008

**Abstract**

As the demand for wireless networks grows, the research community continues to seek methods for improving network performance. On method for improving network throughput involves using *directional antennas* to increase signal gain and/or decrease interference. The physical-layer models used in current networking simulators only minimally address the interaction of directional antennas and radio propagation. This paper compares the models found in popular simulation tools with measurements taken across a variety of links in multiple environments. We find that the effects of antenna direction are significantly different from the models used by the common wireless network simulators.

We propose a parametric model which better captures the effects of different propagation environments on directional antenna systems; we also show that the derived models are sensitive to both the *direction* of signal gain and the *environment* in which the antenna is used. Equally important, we demonstrate how researchers can use inexpensive equipment to record data for their own environments. Although we use sensitive vector signal analyzers in our measurements, we show that using commodity wireless networking cards produces effectively equivalent models. We believe that a combination of the specific model we propose and the process by which we gather data to derive that model will influence the simulated performance of wireless network protocols that rely on directional antennas, providing a more realistic assessment of those protocols. We also offer some general guidance for researchers attempting to use directional antennas to modify a wireless network topology or reduce interference.

## 1 Introduction

Computer network researchers are making use of increasingly sophisticated wireless networking equipment in an effort to design robust wireless networks. While the limitations and problems of modeling wired network devices is both well studied and well known to the networking research community, the use of *wireless* networks introduces additional complexities, such as the effects of radio propagation, that are unfamiliar to many computer scientists. As with the design of most network protocols, much of the work in designing wireless networks uses simulation and models of physical devices to evaluate the design of protocols. Accurately capturing the behavior of the physical layer is essential in that it informs and influences the behavior of the Media Access Control (MAC) layer. This paper examines the models for particular antennas that are being adopted in wireless networks.

Increasingly, networks are using *directional* antennas to improve the throughput or reach of networks [14] or to reduce interference between adjacent networks or from other noise sources.

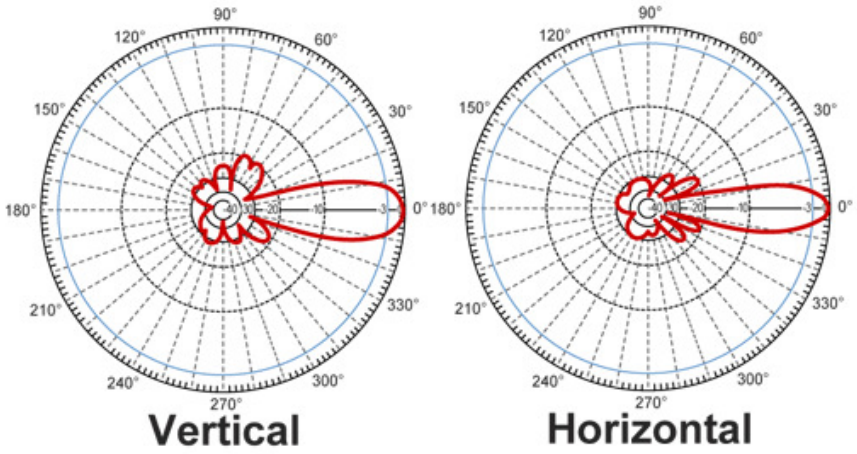


**Figure 1**: Sample directional antenna gain pattern displayed on a polar graph

A more recent development is the use of electronically steerable directional or phase array antennas [10, 5, 16]. These antennas provide better network performance by controlling the radiation pattern of the antenna, increasing the gain (strength of the transmitted and received signal).

Figure 1 shows a common visualization used to understand the antenna gain pattern for a particular highly directional antenna.[1] The pattern shows a predominant main lobe along with a number of "side lobes" interspersed with "nulls" or regions of strongly reduced gain. Fixed or steerable directional antennas provide better network performance by controlling the radiation pattern of the antenna, increasing the gain or alternatively reducing interference by "steering a null" at a radio on the same channel.

In most analytical models, researchers use a very simplified version of these diagrams, typically a simple conic section. Different network simulators model such antennas with different degrees of fidelity. In this paper, we argue that the commonly used models in the most common network simulators make such simplifying assumptions that it is often difficult to draw strong conclusions from the simulations derived using those models.

We demonstrate this using a series of measurements with several different and widely used directional antenna configurations. We then develop a more accurate model based on measurements and intuitions about radio propagation. We argue that this model captures more about the uncertainty of the environment than the specifics of the antenna and that our results should be generally applicable to many different directional antenna patterns with similar gain characteristics.

Our measurement study uses sophisticated measurement equipment, including a $50,000 vector signal analyzer (VSA) and an equally expensive signal generator (VSG). Since the costs of such equipment are prohibitive, we also developed a method that uses inexpensive equipment, such as standard networking cards, to reproduce the data needed for the derived models.

This paper makes the following contributions to the state of knowledge of networking using directional antennas:

[1]This particular example is the 2.4 GHz 19 dBi Die Cast Directional Reflector Grid Wireless LAN Antenna Model: HG2419G by HyperLink Technologies.

- We argue that it is important to characterize directional antennas for the environment in which they are to be used.
- We develop a methodology for producing a parameterized model that better models antennas and is as easy to use as existing models
- Based on our measurements, we offer some observations for research projects using directional antennas:
  - Any algorithm using dynamic beam-steering should try to adapt to the deployed environment rather than relying on prescribed beam patterns.
  - Researchers using directional antennas for *topology control* or interference rejection *via* null-steering should be particularly concerned with the fidelity of their modeling environment.

In the next section of this paper, we go over the basics of radio propagation models to demonstrate the general flavor of the solution we propose. We then describe what the various simulation systems actually model. In §3 we propose our data collection method and in §4 we describe the set of measurements that we use to derive our model. In §5 we analyze that data and in §6 we fully develop our proposed model. Finally in §7, we conclude.

# 2 Background And Related Work

## 2.1 Path Loss Models

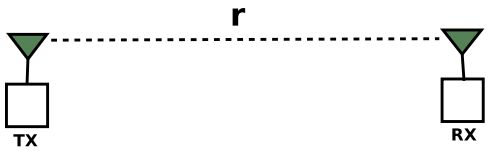


**Figure 2**: Simple path model

Wireless network simulators use a *path loss model* to model the degradation of a transmitted signal; when a signal is too degraded, it cannot be received reliably. Consider the example in Figure 2 with a transmitter and a receiver. Assuming a simplified (i.e., naive) model, energy is propagated in all directions and the energy that actually strikes the receiver would seem to be proportional to the square of the distance between the transmitter and receiver – the signal is attenuated $\propto r^2$. This simple path loss model ignores the significant reflection, scattering, refraction, and absorption effects as RF energy interacts with the earth, the atmosphere, and other smaller features. One of the major effects is *multipath interference*, where the RF waves bounce off objects in the environment and converge at the receiver after having traversed different distances.

The top of Figure 3 shows a schematic of this effect, and this schematic is the basis for the *two ray model* model. In that model, two rays are modeled from the transmitter to the receiver. Because they are electromagnetic waves, they may destructively interfere, leading to a *fade*. Overall, the signal is attenuated the further that it travels. The two-ray model uses a reflection

from the earth and the heights of the transmitter and receiver to indicate the likely signal strength at a given distance. This model is specific to the radio frequency used; Figure 3 is an example of a two-ray calculation from an survey tutorial on antenna propagation models [11] for a 900MHz signal for a 8.7m high transmitter and a 1.6m high receiver; the horizontal axis is a logarithmic scale.

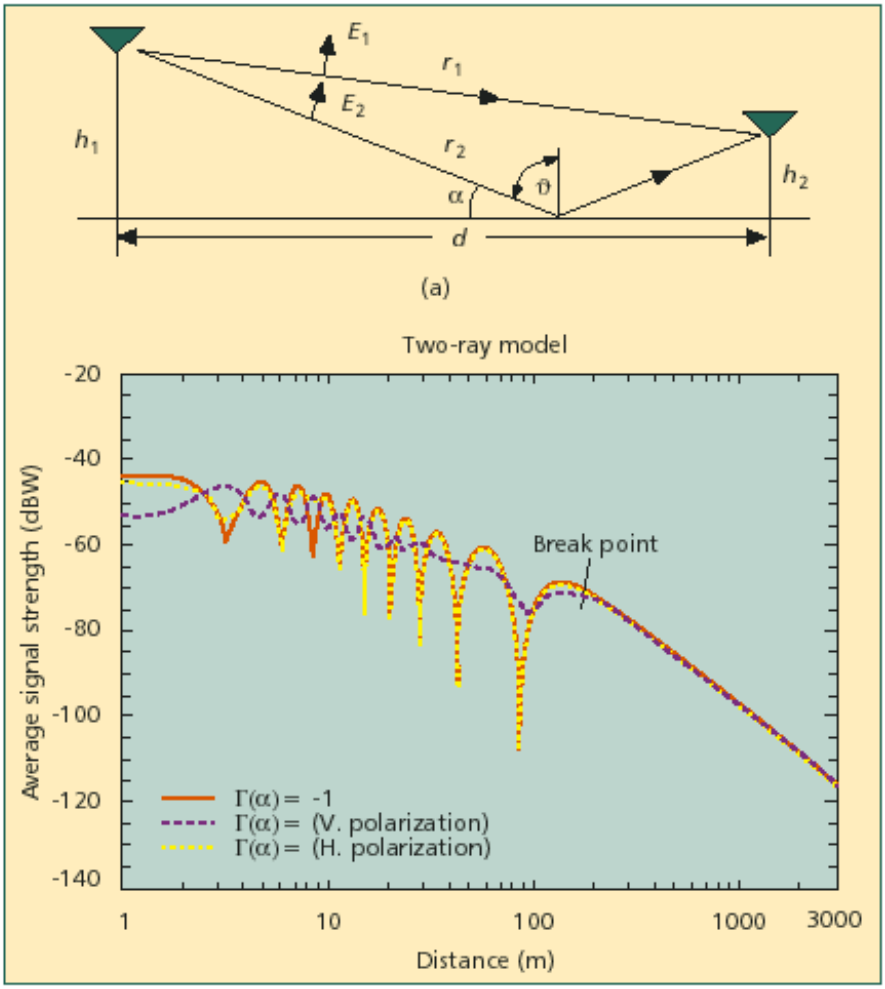


**Figure 3**: Example of two-ray model attenuation

This diagram shows that the signal strength decreases roughly as $r^k, 2 \leq k \leq 4$, but that there is considerable variation over short distances. Other models for such effects are based on fitting empirical measurements rather than *a-priori* analysis. There are general-purpose models such as the Hata / COST231 model and the Longley-Rice model [2, 12], and several specific to the wavelength and operating characteristics of wireless LAN cards [7]. Additionally, the propagation characteristics of indoor environments are sufficiently different from outdoors that there a number of measurement studies [13, 15, 4, 20, 22] and models (See [3], [11] and [8] for excellent surveys).

The preceding work describes relatively large-scale phenomena. In addition to whatever long-range attenuation there may be, there is also small-scale fading, which is the result of

multipath interference and occurs at the scale of single wavelengths. Though such interference can theoretically be predicted analytically, it requires that the environment be known with a level of detail that is generally impractical [19, 18].

A common way of address such situations is through *statistical* fading models. Rather than determine the signal strength at any exact place or time, it is modeled as a random variable with a known distribution. In general, the distributions are fairly well-established, but the parameters are very environment-specific (see e.g. [6]). There are several common models, among them *Rayleigh fading* which assumes that there are many comparable multipath signals, and *Rician fading* which assumes a less "cluttered" environment in which line-of-site paths are more important.

Our model for directional antennas adopts a similar approach to the empirical model and the Rayleigh fading model – we use empirical measurements to identify the characteristics of the random or stochastic process. Where we differ is that our model is primarily concerned with effects on directionality.

## 2.2 Directional Models

The simulators commonly used in networking research do not consider antenna directionality and radio propagation as interacting variables. This paper considers three widely-used simulators, *OpNet*, *QualNet*, and *NS-2*. Each one supports several models of radio propagation, but they all follow the same general model with regard to antenna gain: For any two stations $i$ and $j$, the received signal strength is computed according to the general form of equation 1:

$$\text{Received Power} = P_{tx} * G_{tx} * |PL(i,j)| * G_{rx} \tag{1}$$

The received power $P_{rx}$ is the product of the transmitted power $P_{tx}$, the transmitter's gain $G_{tx}$, the magnitude of path loss between the two stations $|PL(i,j)|$, and the receiver's gain $G_{rx}$.

The transmitter and receiver gains are essentially constants in the case of omnidirectional (effectively isotropic in the azimuth plane) antennas. For directional antennas, gain is an antenna-specific function of the direction of interest. For some given zenith $\phi$, azimuth $\theta$, and an antenna-specific characterization function $f_{a\ tx}()$, the power transmitted in that direction is given by equation 2:

$$\text{Gain in direction}(\phi,\theta) = f_a(\phi,\theta) \tag{2}$$

$$\text{Combined gain} = f_a(\phi,\theta) * f_b(\phi',\theta') \tag{3}$$

Correspondingly, the receiver gain is modeled by a (potentially different) function of the direction from which the signal is received. Besides being a source of interference for a dominant signal, the energy traveling along secondary paths also carries signal. Network simulators model the path loss using the difference in angles between the transmitter and receiver. However, if one of the weaker signals for a transmitter happens to be aligned with a high-gain direction of a receiving antenna, the received power from that path can be greater than that of the primary path. Thus in environments with significant multipath, the gain cannot be determined based solely on a single direction. This is easier to understand using figure 4, which combines a transmitter (on the left) and a receiver (on the right).

In this figure, the transmitter gain is indicated by the (large) gain of the antenna pattern; the receiver gain is indicated by the (much smaller) gain from the "side-lobe" that is linearly

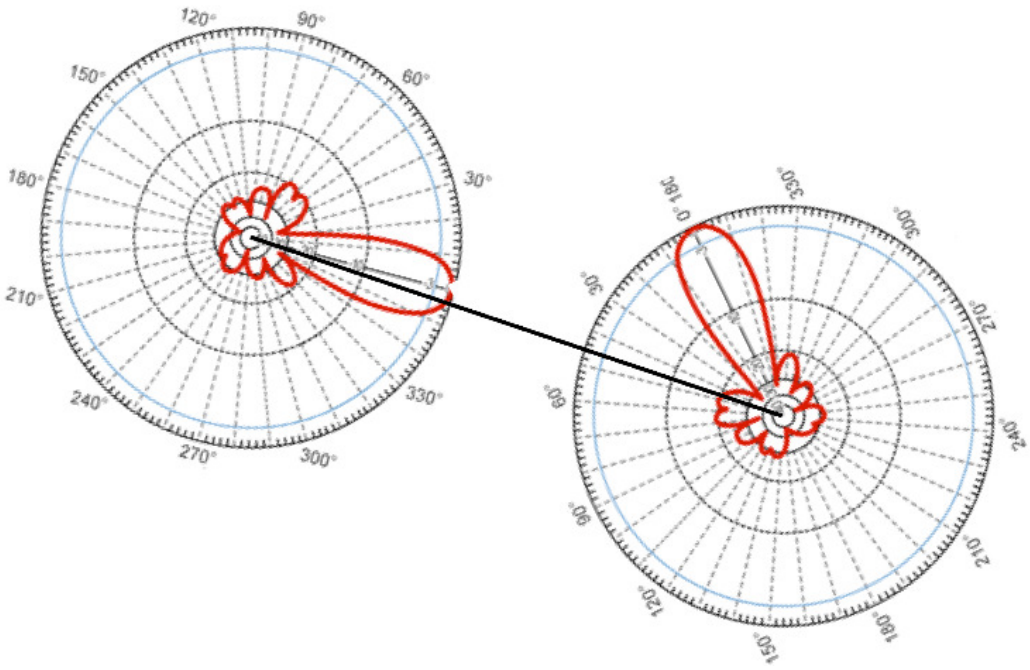


**Figure 4**: Illustration of the common path loss model for directional antennas

located between transmitter and receiver. The complex-valued path loss, $PL(i, j)$, is related to the length of the dark line separating the transmitter and receiver.

The above models describe the power emitted in or received from a single direction. In reality, the transmitter's power is radiated in all directions, and the receiver aggregates power (be it signal or noise) from all directions. Although the simulators we are considering assume that the single direction of interest for each station is precisely toward the other station, we can generalize equations 1 and 3 to the case where there are multiple significant signal paths:

$$P_{rx} = \sum_{l \in \text{paths}} P_{tx} * f_a(\phi_l, \theta_l) * PL_l(i, j) * f_b(\phi'_l, \theta'_l) \tag{4}$$

In Equation 4, note that that $P_{rx}$ is not necessarily all "signal". It may be the case that only one signal is decodable and the others destructively interfere in which case equation 5 is a better model:

$$P_{rx} = \max_{l \in \text{paths}} P_{tx} * f_a(\phi_l, \theta_l) * PL_l(i, j) * f_b(\phi'_l, \theta'_l) \tag{5}$$

Both of these models assume that there is some way to describe available paths that a signal may take. As with the Rayleigh and Rician fading models, it may be possible to build a parameterized model of those paths for "cluttered" and "uncluttered" environments. This is the approach we take, using measured data to determine the model.

With any of the three simulators we consider, the user has the freedom to provide any type of mapping between gain and angle. This means that the user could conceivably make

measurements with their desired hardware in their desired environment, much as we have done, and then install this as the pattern. However, even though the antenna can conceivably be modeled arbitrarily well, we will show that the *directionality of the signal* is an effect of the interaction between antenna and environment and that modeling both in isolation, however well, misses significant effects. We propose a combined empirical model which attempts to account for both the pattern of the antenna and the deviation from this pattern due to environmental effects.

# 3 Method

In this section we will describe the method we devised for deriving empirical models for antenna patterns using commodity hardware and address any reservations about their accuracy by providing a means for equipment calibration.

## 3.1 Data Collection Procedure

We use two laptops, one receiver and one transmitter. Each is equipped with an Atheros-based MiniPCI-Express radio which is connected to an external antenna using a U.Fl to N pigtail adapter and a length of LMR-400 low-loss antenna cable. The receiver laptop is connected to a 7 dBi omnidirectional antenna on a tripod approximately two meters off the ground. The transmitter laptop is connected to the antenna we intend to model on a tripod 100 feet from the receiver and also two meters off the ground. The transmitter tripod features a geared triaxial head which allows precise rotation.

The transmitter radio is put in 802.11x ad hoc mode on the least congested channel. The transmitter's ARP table is manually hacked to allow it to send UDP packets to a non-existent receiver. The receiver is put in monitor mode on the same channel and logs packets with tcpdump. Finally, both the receiver and transmitter must have antenna diversity disabled. With the equipment in place, the procedure is as follows: For each 5 degree position about the azimuth, send 500 un-acknowledged UDP packets. Without intervention otherwise, due to MAC-layer retransmits, each will be retried $k$ times (where k is radio-vendor and/or driver implementation specific), resulting in $k * 500$ measurements.

During the experiment, the researchers themselves must be careful to stay well out of the near-field of the antennas and to move to the same location during runs (so that they, in effect, become a static part of the environment). If additional data is desired for a given location, multiple receivers can be used, provided the data from them is treated separately (as each unique path describes a unique environment).

## 3.2 Commodity Hardware Should Suffice

To ensure that it is safe to use commodity 802.11x-based hardware to measure antenna patterns, we calibrate the sensitivity of our radios and analyze losses in the packet-based measurement platform.

In the process of collection, some packets will be dropped due to interference or poor signal. In our experience, the percentage of dropped frames *per angle* is very small: the maximum lost frames per-angle in our datasets is on the order of 5%, with less than 1% lost being more common (the mean is 0.01675%). Moreover, the correlation coefficient between angle and loss

percentage is -0.0451, suggesting that losses are uniformly distributed across angles. Given that we have taken 4000 samples in each direction ($k = 8$ for our configuration), noise in our measurements due to packet loss is negligible.

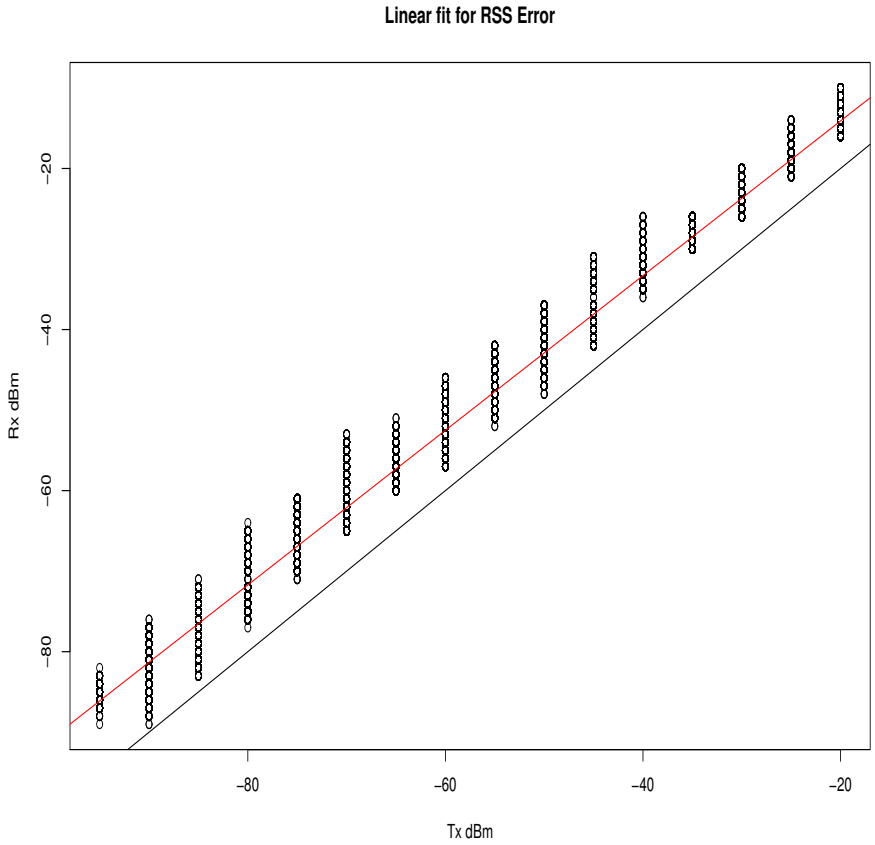


**Figure 5**: Linear fit to RSS error observed from commodity cards during calibration.

To get an idea of how accurate our commodity radios are in measuring received signal strength (RSS), we directly connected each of four radio cards (all Atheros-based Lenovo-rebranded Mini-PCI express) to an Agilent E4438C VSG. The VSG was configured to generate 802.11 frames and the laptop to receive them. For each of the four cards we collected many samples while varying the transmit power of the VSG between -20 dBm and -95 dBm (lower than the receive sensitivity threshold of just about any commodity 802.11 radio) on 5 dBm increments. The resulting data is plotted in figure 5 along with a linear fit with a slope of 0.9602 and adjusted R-squared value of 0.9894 (indicating a strong fit to the data). The commodity radios perform remarkably well in terms of RSS measurement. To correct for the minor error they do exhibit, we use the slope of this fit to adjust our measurements, dividing each measurement by the slope value.

| Label | Environment | Line of Sight? | Distance (ft) | Samples | Loss Rate (%) |
|---|---|---|---|---|---|
| Parabolic-Outdoor-A | Open Field on Campus | Yes | 100 | 214471 | 24.81 |
| Parabolic-Outdoor-B | Empty Floodplain | Yes | 100 | 258876 | 7.05 |
| Parabolic-Indoor-A | Laboratory | Yes | 100 | 267092 | 2.21 |
| Parabolic-Indoor-B | Office Building | Yes | 200 | 268935 | 10.41 |
| Parabolic-Indoor-C | Office Building | No | 50 | 283104 | 5.12 |
| Parabolic-Reference | Empty Floodplain | Yes | 100 | 219 | N/A |
| Patch-Outdoor-A | Open Field on Campus | Yes | 100 | 455952 | 12.44 |
| Patch-Outdoor-B | Empty Floodplain | Yes | 100 | 278239 | 4.99 |
| Patch-Indoor-A | Laboratory | Yes | 100 | 290030 | 2.21 |
| Patch-Indoor-B | Office Building | Yes | 200 | 265593 | 7.40 |
| Patch-Indoor-C | Office Building | No | 50 | 278205 | 2.65 |
| Patch-Reference | Empty Floodplain | Yes | 100 | 219 | N/A |
| Array-Outdoor-A | Open Field on Campus | Yes | 100 | 475178 | N/A |
| Array-Indoor-A | Office Building | Mixed | Varies | 2672050 | N/A |
| Array-Indoor-B | Office Building | Mixed | Varies | 2708160 | N/A |
| Array-Reference | Open Urban Area | Yes | 5 | 360 | N/A |

**Table 1**: Summary of data sets

# 4 Measurements

In this section we will explain the datasets we collected, discuss our normalization procedure, and give some high-level statistical characterization of the data.

## 4.1 Experiments Performed

In order to derive an empirical model that better fits real world behavior, we collected data in several disparate environments with three different antennas. A high level summary of these datasets is in table 1. With the exception of the reference patterns, all of the measurements were made with commodity hardware by sending many measurement packets between two antennas and logging received signal strength (RSS) at the receiver. The three antenna configurations used include - a HyperLink 24dBi parabolic dish with an 8-degree horizontal beam-width, a HyperLink 14dBi patch with a 30 degree horizontal beam-width, and a Fidelity Comtech Phocus 3000 8-element uniform circular phased array with a main-lobe beam-width of approximately 52 degrees. This phased array functions as a switched-beam antenna and can form this beam in one of 16 directions (on 22.5 degree increments around the azimuth). For the HyperLink antennas, we used the same antenna in all experiments to avoid intra-antenna variation due to manufacturing differences.

In addition to the in-situ experiments, we have a "reference" data set for each configuration. The Array-Reference data set was provided to us by the antenna manufacturer. Because HyperLink could not provide us with data on their antennas, Parabolic-Reference and Patch-Reference were derived using an Agilent 89600S VSA and an Agilent E4438C VSG in a remote floodplain[2] (see figure 10 for a photo of the receiver-side of this setup).

[2]We were unable to aquire access to an anechoic chamber in time for this study, but would like to make use of one in future work, for even cleaner reference measurements.

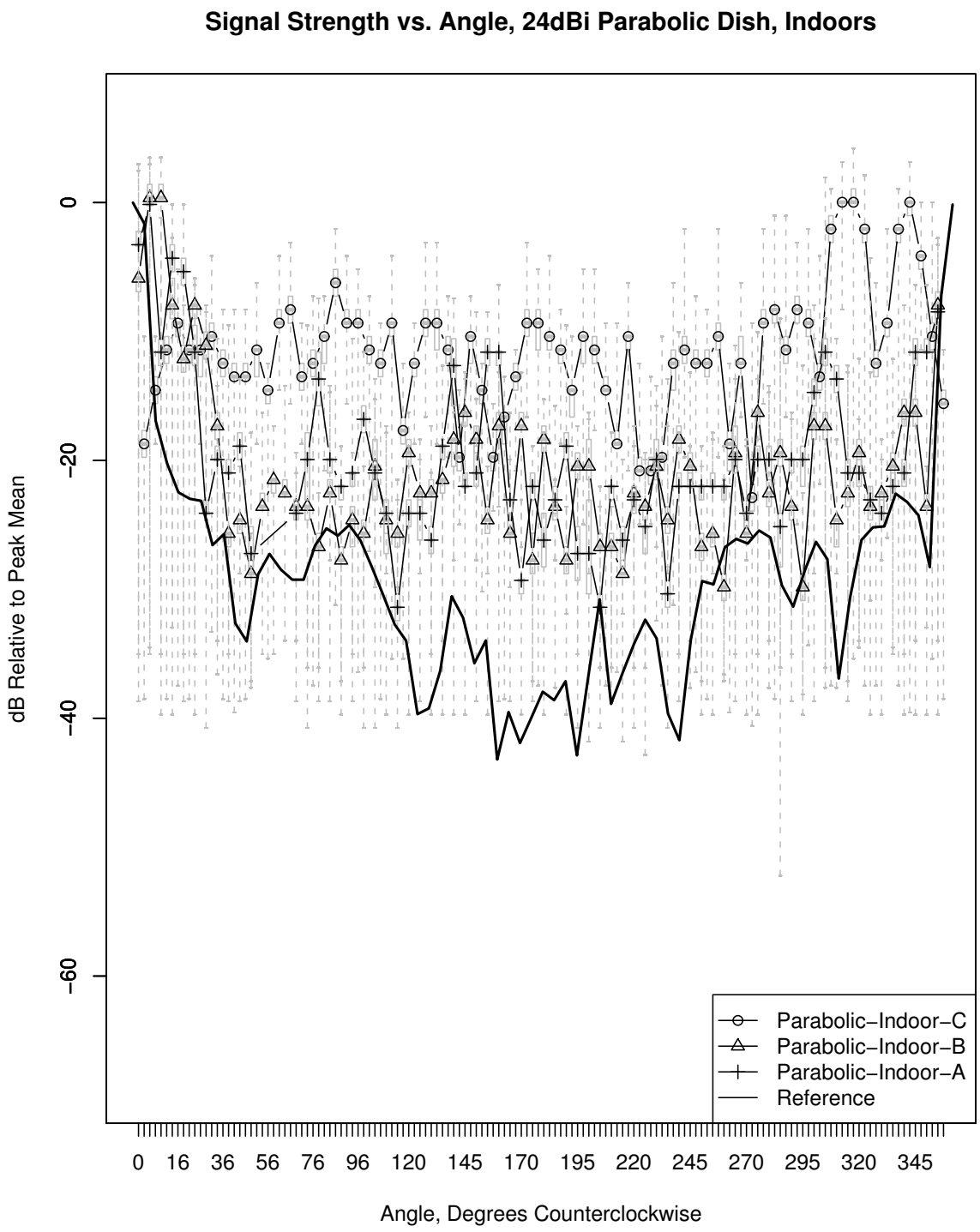


**Figure 6**: Comparison of signal strength patterns across different environments and antennas: Parabolic dish indoor environments.

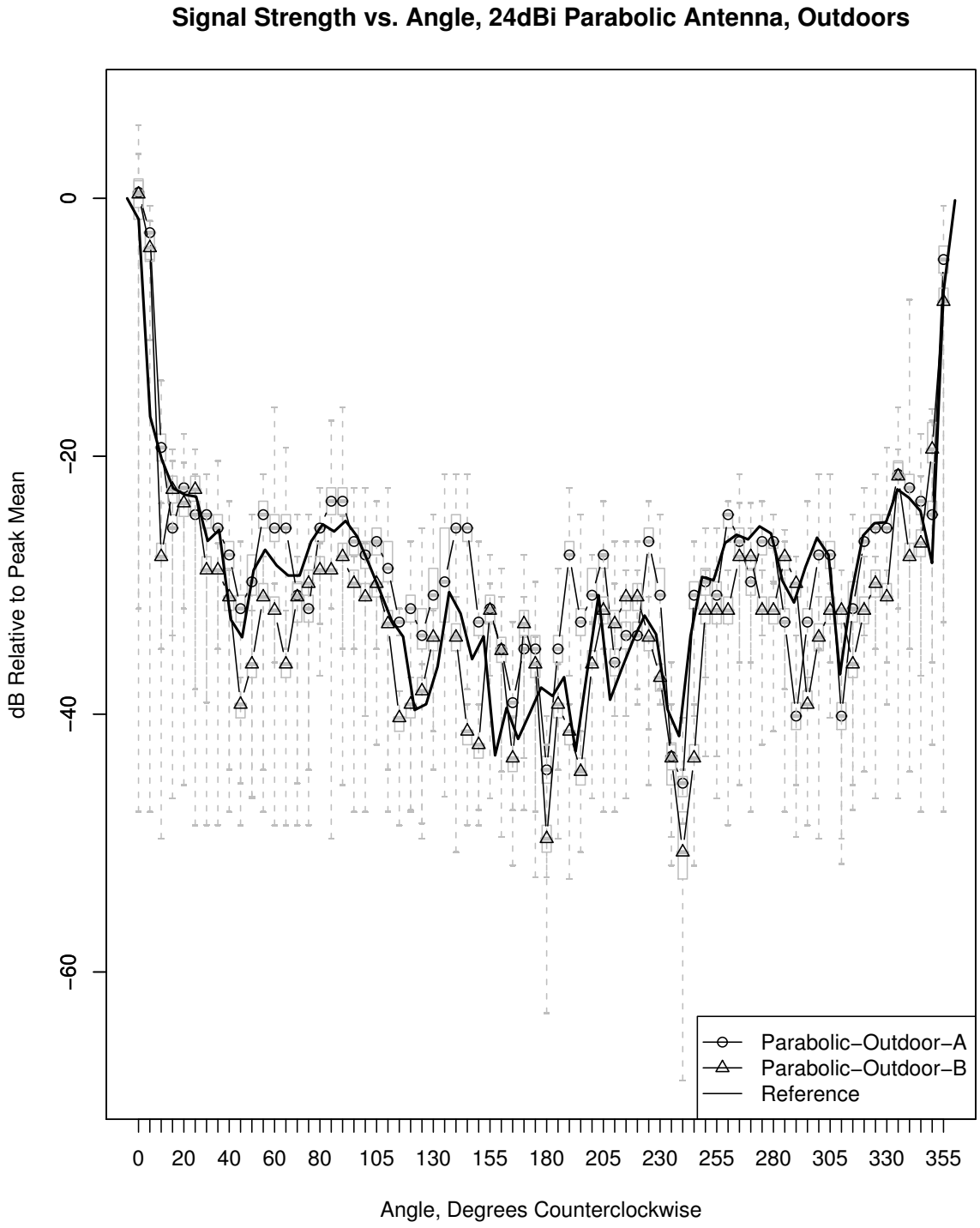


**Figure 7**: Comparison of signal strength patterns across different environments and antennas: Parabolic dish outdoor environments.

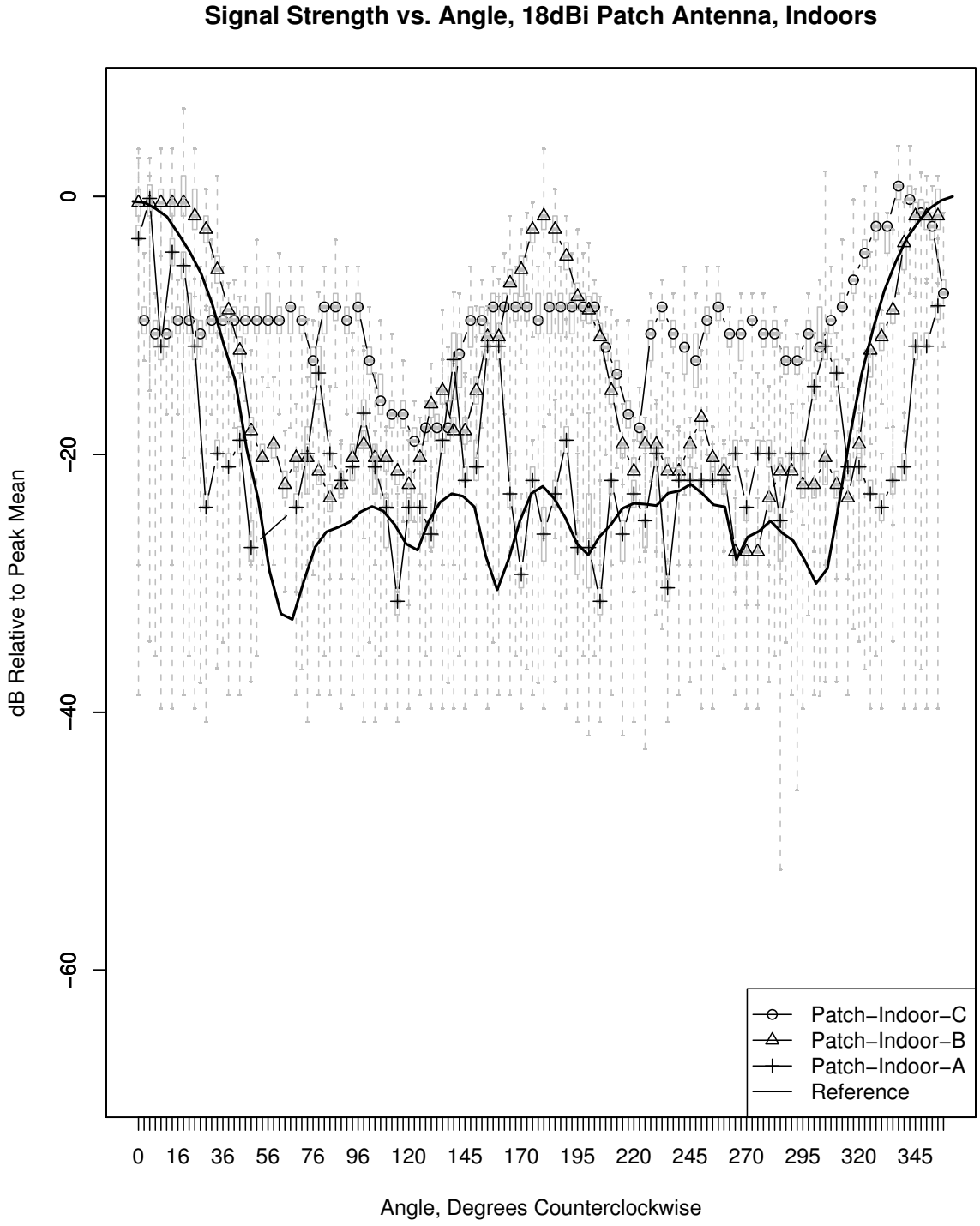


**Figure 8**: Comparison of signal strength patterns across different environments and antennas: Patch panel indoor environments.

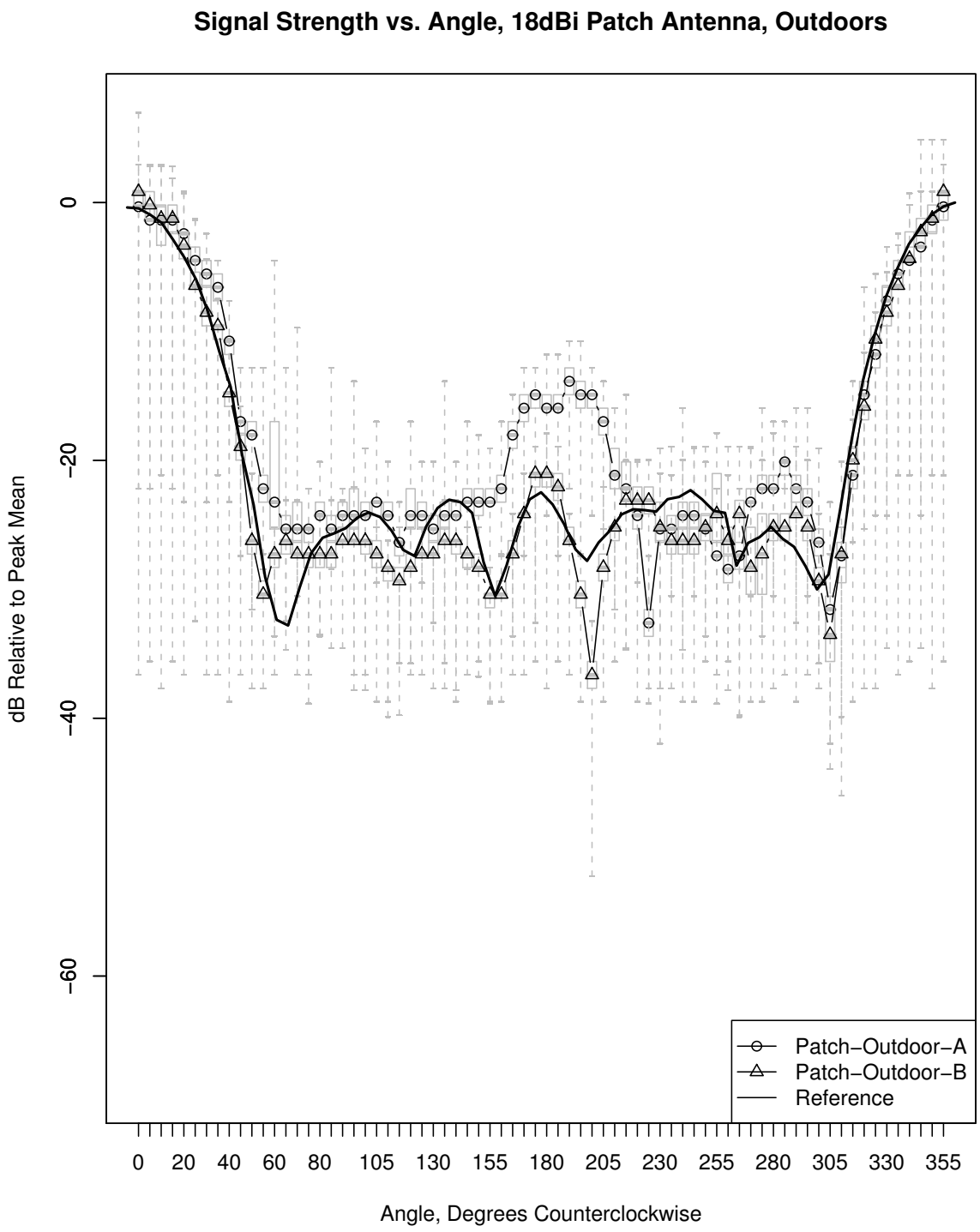


**Figure 9**: Comparison of signal strength patterns across different environments and antennas: Patch panel outdoor environments.

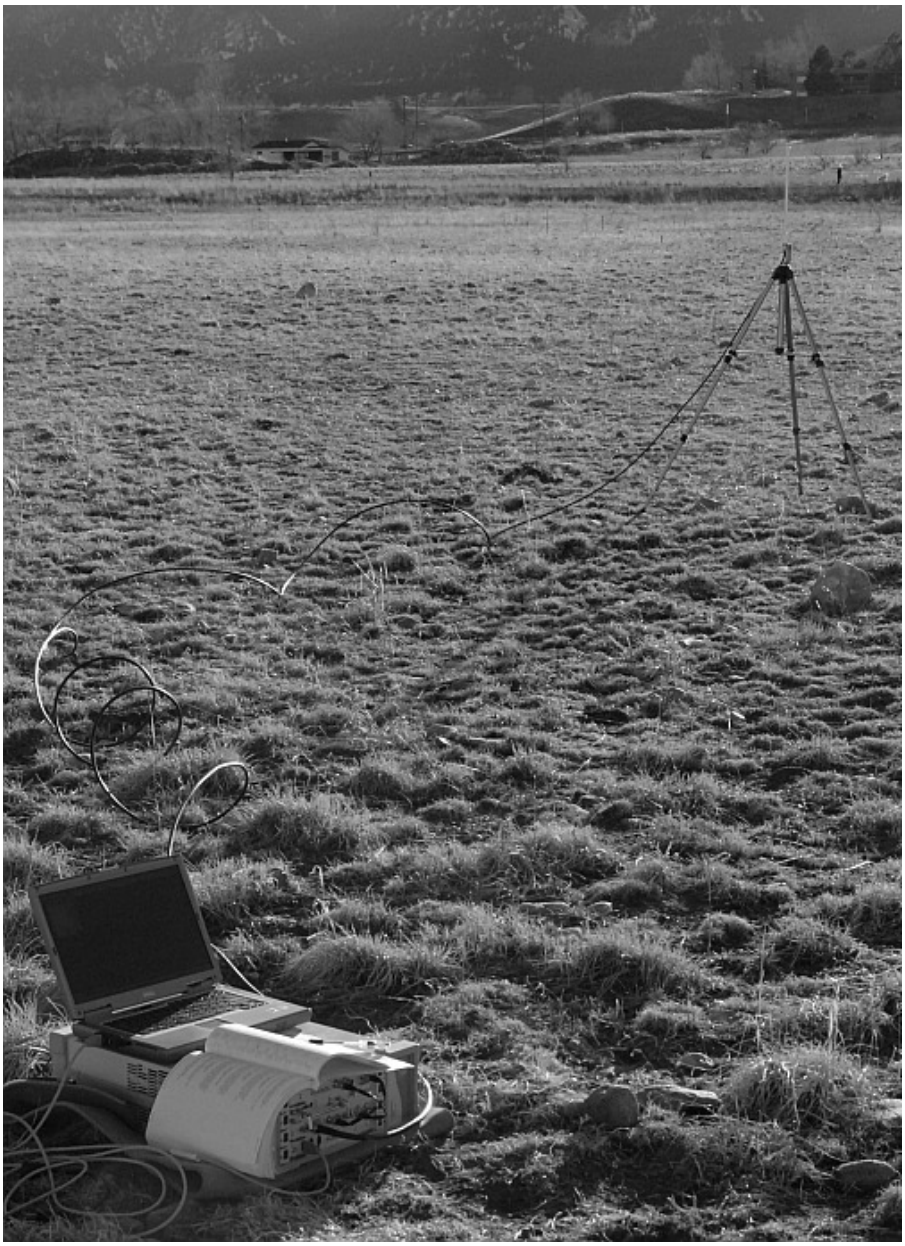

**Figure 10**: Receiver side of measurement setup in floodplain

**Figure 11**: Floorplan of office building used in Array-Indoor-A, Array-Indoor-B, Patch-Indoor-B, Patch-Indoor-C, Parabolic-Indoor-B, and Parabolic-IndoorC.

Following is a brief description of each of the experiments[3]:

- **Parabolic-Outdoor-A, Patch-Outdoor-A** – A large open field on the University of X campus was used for these experiments. The field is roughly 500-feet on a side and is surrounded by brick buildings on two of the four sides. Although there is line of sight and little obstruction, the surrounding infrastructure makes this location most representative of an urban outdoor deployment.

- **Parabolic-Outdoor-B, Patch-Outdoor-B** – A large University-owned floodplain on the edge of town was used for our most isolated data sets. The floodplain is flat, recessed, and is free from obstruction for nearly a quarter mile in all directions. This location is most representative of a rural backhaul link.

- **Array-Outdoor-A** – The same open field is used as in the Parabolic-Outdoor-A and Patch-Outdoor-A data sets. The collection method here differs from that described in section 3. A single phased array antenna is placed approximately 100 feet away from an omni-directional transmitter. The transmitter sends a volley of packets from its fixed position as the phased array antenna electronically steers its antenna across each of its 16 states, spending 20 ms in each state. Several packets are received in each directional state. The phased array antenna is then manually rotated in 10 degree increments while the omni-directional emitter remains fixed. The same procedure is repeated for each of 36 increments. Moving the emitter changes not only the angle relative to the antenna but also the nodes' positions relative to their environment. To address this confound, each physical position is treated as a separate experiment. This means that the number of

[3]We will release our entire data set to the community[1] prior to publication.

angles *relative to the steered antenna pattern* is limited to the number of distinct antenna states (16). The tx-power of the radio attached to the directional antenna was turned down to 10dBm to produce more tractable noise effects (for the purpose of modeling small-scale behavior the default EIRP is much too high).

- **Parabolic-Indoor-A and Patch-Indoor-A** – For this data set we used the University of X Systems Lab. The directional transmitter was positioned approximately 20 feet from the receiver in a walkway between cubicles and desks. This is our most cluttered environment.

- **Parabolic-Indoor-B, Parabolic-Indoor-C, Patch-Indoor-B, and Patch-Indoor-C** – An indoor office space was used for this set of tests. See figure 11 for the floor-floorplan of this office space. Two receivers were used here: one with line of sight and one without line of sight, placed amidst desks and offices.

- **Array-Indoor-A and Array-Indoor-B** – Seven phased array antennas are deployed in the same 25x30m indoor office space used for Parabolic-Indoor-B, Parabolic-Indoor-C, Patch-Indoor-B, and Patch-Indoor-C. Data from two of the seven antennas are analyzed here. Each antenna electronically steers through its 16 directional states, spending 20 ms at each state. Two mobile omni-directional transmitters move through the space and transmit 500 packets at 44 distinct positions. For each packet received by a phased array, the packet's transmission location and orientation is recorded (i.e., which of the four cardinal directions was the transmitter facing) along with the directional state in which the packet arrived and the RSSI value.

- **Parabolic-Reference and Patch-Reference** – The large flood-plain is used here. An Agilent VSA is connected to the omni-directional receiver and makes a 10-second running average of power samples on a specific frequency (2.412 GHz was used). Three consecutive averages of both peak and band power are recorded for each direction. The directional transmitter is rotated in five degree increments and is connected to a VSG outputting a constant sinusoidal tone at 25 dBm on a specific frequency. Before, after, and between experiments we made noise floor measurements and as a post-processing step, we have subtracted the mean of this value (-59.61811 dBm or 0.0011 $\mu$W) from the measurements.

## 4.2 Normalization

Our first task in comparing data sets is to come up with a scheme for normalization so that they can be compared to one another directly. For each data set, we find the mean peak value which is the maximum of the mean of samples for each discrete angle. This value is then subtracted from every value in the data set. The net effect is that the peak of the measurements in each data set will be shifted to zero.

## 4.3 Characterization

### 4.3.1 Error relative to the reference

Figures 6 through 9 show the normalized measured in-situ patterns and their corresponding (also normalized) reference patterns. Recall that the reference pattern is generated and recorded by calibrated signal processing equipment and the measured data is collected using commodity

802.11 cards. As can be clearly seen there is much variation in the measured patterns and in how much they differ from the reference (which we would typically classify as error). As we would expect, the measurements in outdoor environments exhibit less noise due to less clutter, but still deviate from the reference on occasion. As a further confirmation that our measurement process works well, notice how well Parabolic-Outdoor-B and Patch-Outdoor-B (figures 7 and 9) correlate with the reference pattern (recall that these experiments were done in the same floodplain as the reference, indicating that the commodity hardware can compete with the expensive specialized equipment in a similar environment).

### 4.3.2 Distribution of Error

Our foremost question in characterization is: *is there a straight-forward explanation for error in the measured patterns*? Figure 12 provides a CDF of all error for each antenna. The three antennas provide similar error distributions, although offset in the mean. The Array data is the most offset from the others (presumably because its reference pattern is theoretical rather than measured) and exhibits some bimodal behavior. The Patch measurements are closest to the reference, showing a large kurtosis about zero.

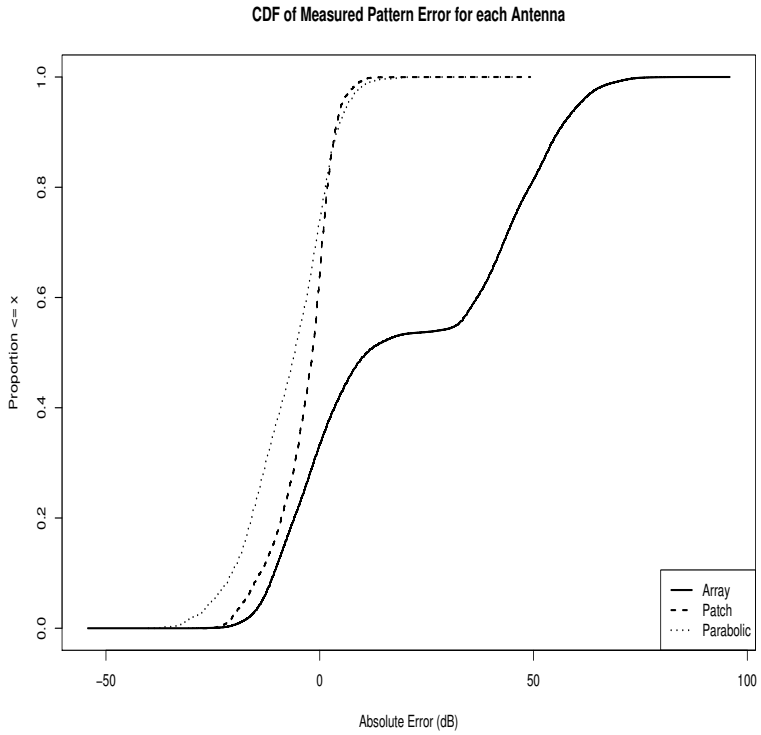


**Figure 12**: Cumulative Density Functions for the error process (combined across multiple traces) for each antenna type.

### 4.3.3 Patterns in error based on angles

Clearly, the antennas have different error characteristics. However, within each antenna, and within each data set, it might be that the error in a given direction is correlated with that in other directions – if this were true, we could use a single or small set of probability distributions to describe the error process in a given environment, with a given antenna.

We used a Shapiro-Wilkes test on the per-angle error for each data set. The resulting p-values are well under the $\alpha = 0.05$ threshold, and in all cases we can reject the null-hypothesis that the error is normally distributed; this means that standard statistical tests (and regression models) which assume normality can not be used. Thus, we choose to use nonparametric statistical tests. A pairwise Mann-Whitney U-test can be used to determine which pairs of samples grouped on some criterion (in our case angle) are drawn from the same distribution. Figure 13 plots a heatmap showing the interaction between angles for a representative data set. Remarkably, all of our traces produce heatmaps with similar trends: in the majority of pairs we reject the null hypothesis that their error process is drawn from the same distribution. However, for angles near zero, we are unable to reject this hypothesis. This observation, that *measurements where the main-lobe of the directional antenna is pointed at the receiver may exhibit correlated error processes*, motivated another series of tests.

To further explore "possibly well behaved" error processes about the main lobe, we applied a Kruskal-Wallis rank-sum test to two scenarios:

1. For angles near zero, are batches with the same antenna (but different environments) equivalent?

2. For angles near zero, are batches with the same environment (but different antennas) equivalent?

For 1, the null hypothesis is soundly rejected for all combinations. In fact, the maximum p-value found is 1.990343e-40. For 2, the results still point strongly towards rejection (mean p-value = 0.0082), however there is one outlier - in the case of 355 degrees in the laboratory environment, we achieve a p-value of 0.2097. One outlier, however, is not sufficient to derail the overwhelming evidence that neither antenna configuration nor environment alone is sufficient to account for intra-angle variation in error - even in the more seemingly well-behaved cone of the antenna main-lobe.

## 4.4 Observations

There are several qualitative points which are worth bringing out of this data: (1) In the indoor environments, none of the measured traces tracks the reference signal at all closely; (2) In all environments, there is significant variation between data sets; (3) The maximum signal strength is generally realized in *approximately* the direction of maximum antenna gain, but directions of low antenna gain often do not have correspondingly low signal strength. This means that *no system for interference mitigation can safely rely on pre-determined antenna patterns.*

# 5 A New Model of Directionality

We began this paper with the observation that path loss and antenna gain are typically regarded as orthogonal components of the power loss between transmission and reception (Eq.s 1 - 3).

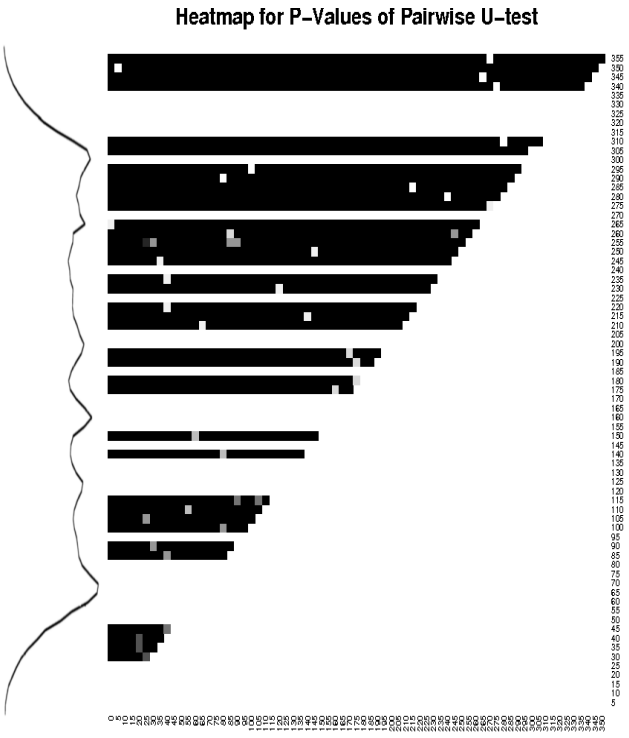


**Figure 13**: Heatmap of p-values for the Mann-Whitney U-test which was run pair-wise against the error from the reference pattern in each angle. This plot, which is for Patch-Indoor-A, was chosen as a representative. *All traces showed similar trends.* Darker values indicate very small p-values, meaning that the null-hypothesis can be rejected with confidence. In this case, the null-hypothesis is that the samples come from the same distribution. The Patch reference pattern is provided on the left for reference.

In this section, we evaluate the *best case* accuracy of this approach, and suggest a new model based on the limitations identified.

### 5.1 Limitations of Orthogonal Models

This section subsection formalizes the orthogonal antenna gain / path loss model and analyzes the error associated with it. If transmit power and path loss do not vary with antenna angle, the received power relative to antenna angle can be modeled as:

$$\widehat{P_{rx}} = \beta_0 * f(\phi, \theta) \tag{6}$$

This paper uses the convention of designating constants to be estimated (parameters) as $\beta_0 \ldots \beta_n$. In this case, $\beta_0$ is a constant combining the path loss – however calculated – and the gain of the non-rotating antenna. $f(\phi, \theta)$ is a function describing the gain of the other antenna relative to the signal azimuth $\theta$ and zenith $\phi$. Without loss of generality, we will assume that the antenna being varied is the receiver, and that the zenith, $\phi$, is fixed.

To evaluate the accuracy of this model, we start by finding the estimate $b_0$ for $\beta_0$ which minimizes the sum of squared error (SSE). In effect, this is assuming the *best possible path loss estimate*, without specifying how it is determined. If the function $f()$ correctly describes the antenna, and if path loss and antenna gain are in fact orthogonal components of the received signal strength, then the remaining error should be *randomly* distributed about 0.

Figures 14 through 19 depict the error of this *orthogonal model* for several data sets. There are several qualitative observations to be made: First and most importantly, *the error value is not uniformly random, but rather correlated with direction.* The variability within any given direction is less than that for the data set as a whole. Second, the error is significant. In the worst states, the *mean error* is between 8 and 10 dB, in either direction. Third, the model overestimates signal strength in the directions where the gain is highest, and underestimates in the directions where the gain is lowest. That is, *the difference in actual signal strength between peaks and nulls is less than the antenna in isolation would produce.* This has significant implications for systems that use null-steering to manage interference.

The data in figures 18 and 19 is aggregated from 36 distinct physical configurations. In each configuration, the directional receiver was (electronically) rotated in 22.5 degree increments, and between configurations, the omnidirectional emitter was physically moved around the receiver by ten degrees. A consequence of this method is that these 10 degree changes represent not only a change of the angle between the emitter and the antenna, but also a change of location with the attendant possibility of fading effects. To account for this, we consider each of the 36 configurations individually. This gives less angular resolution, but also fewer confounds. Figure 5.1 displays each configuration as a separate line. The model accuracy is fairly consistent: The residual standard error of the aggregate is 8 dB, and the individual cases range from 5.74 dB to 11.4 dB with a mean of 7.6 dB.

This section presents the *best possible case* of the orthogonal model: The path loss value used for each data set was the lowest-error fit for that specific data, and the antenna patterns ($f(\theta)$) for the patch and parabolic antennas were measured using the specific individual antenna in question. Note also that error patterns differ from environment to environment: One could derive an ex post facto $f()$ to eliminate the error in single data set, but it would not be applicable to any other.

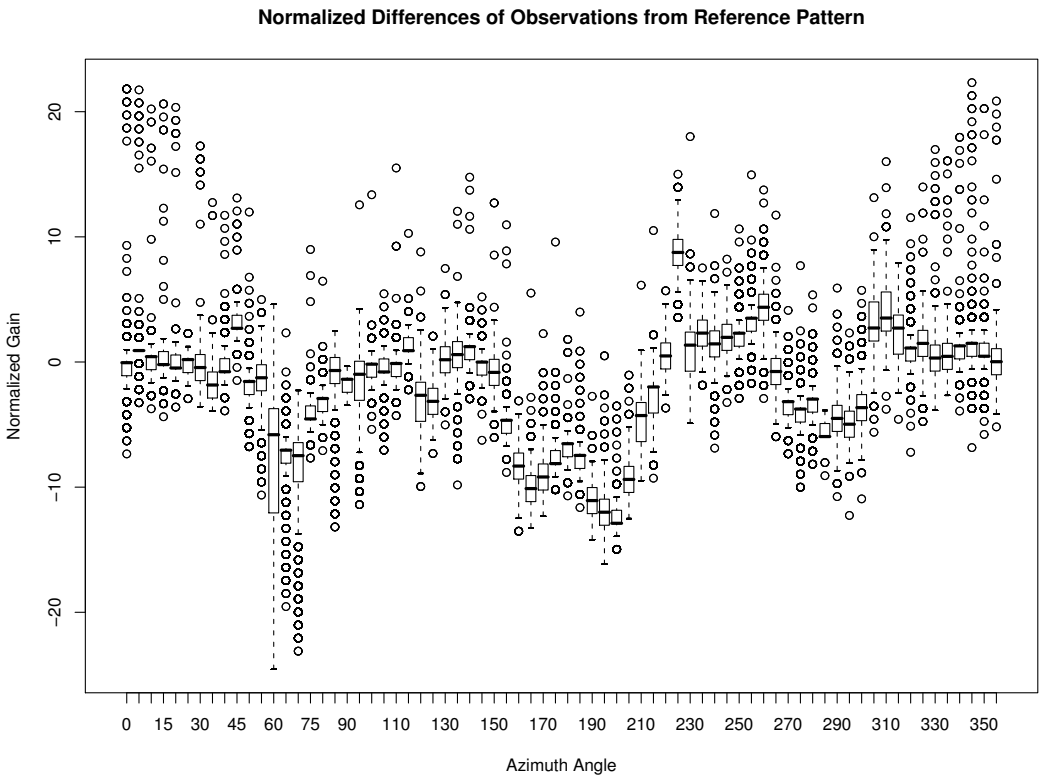


**Figure 14**: Differences between the orthogonal model and observed data in dB: $\hat{P_{rx}} - P_{rx}$: Patch-Outdoor-A

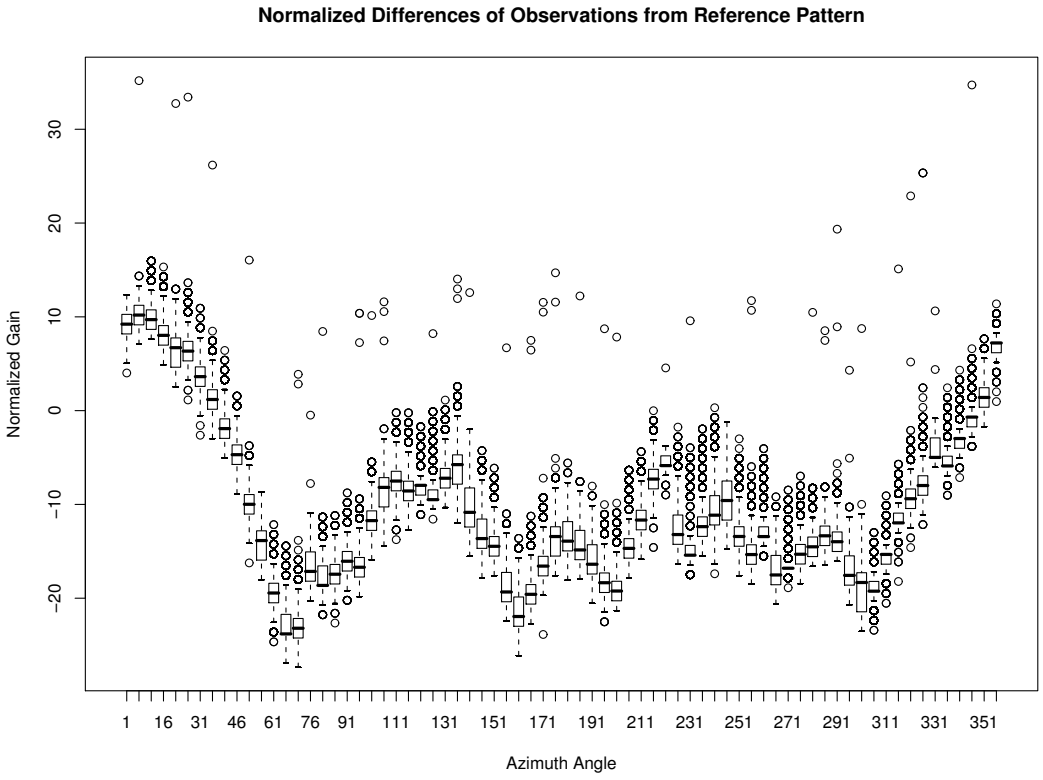


**Figure 15**: Differences between the orthogonal model and observed data in dB: $\hat{P_{rx}} - P_{rx}$: Patch-Indoor-B

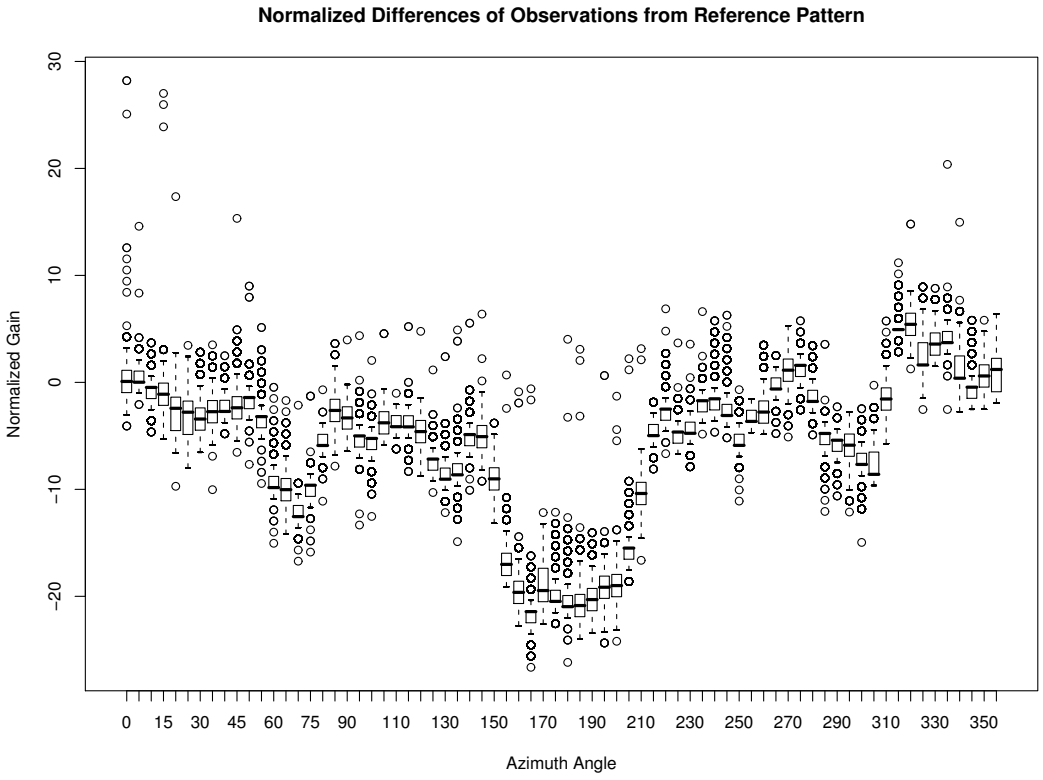


**Figure 16**: Differences between the orthogonal model and observed data in dB: $\hat{P_{rx}} - P_{rx}$: Patch-Indoor-C

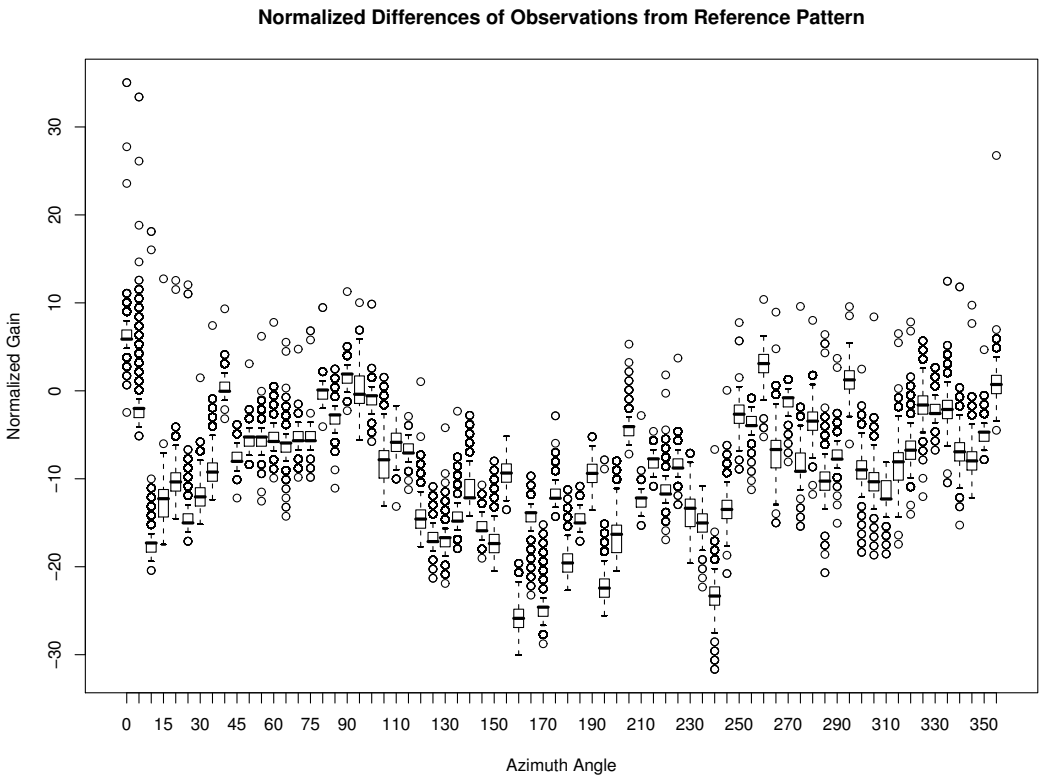


**Figure 17**: Differences between the orthogonal model and observed data in dB: $\hat{P_{rx}} - P_{rx}$: Parabolic-Indoor-C

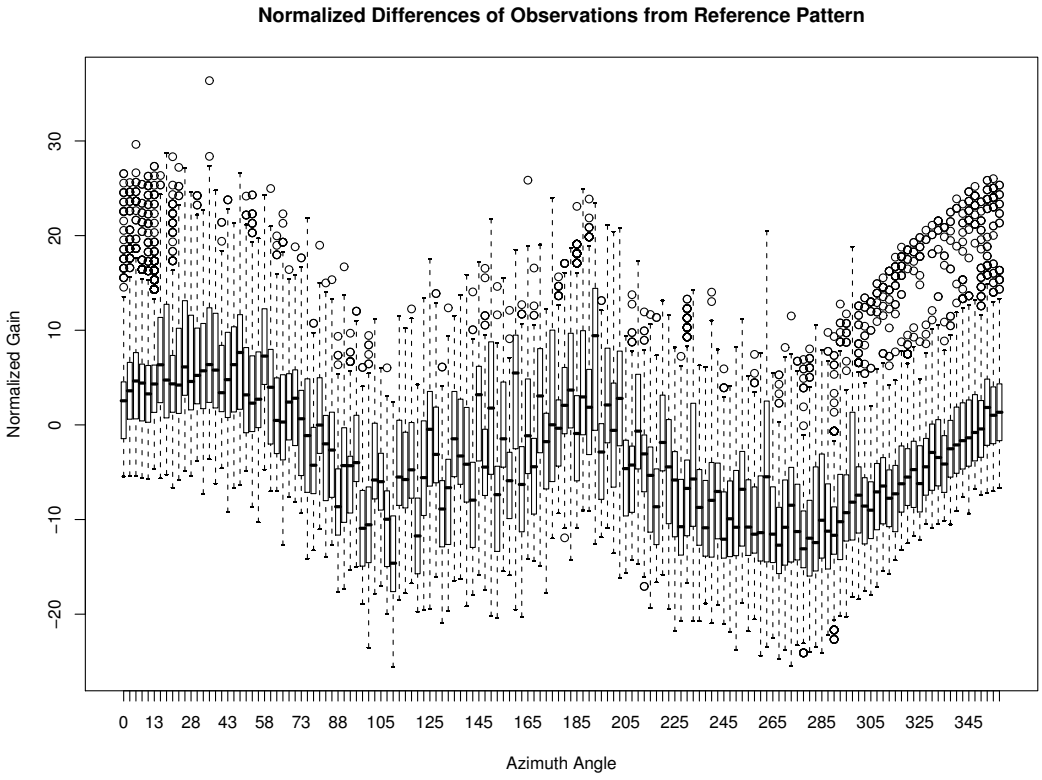


**Figure 18**: Differences between the orthogonal model and observed data in dB: $\hat{P_{rx}} - P_{rx}$: Array-Outdoor-A

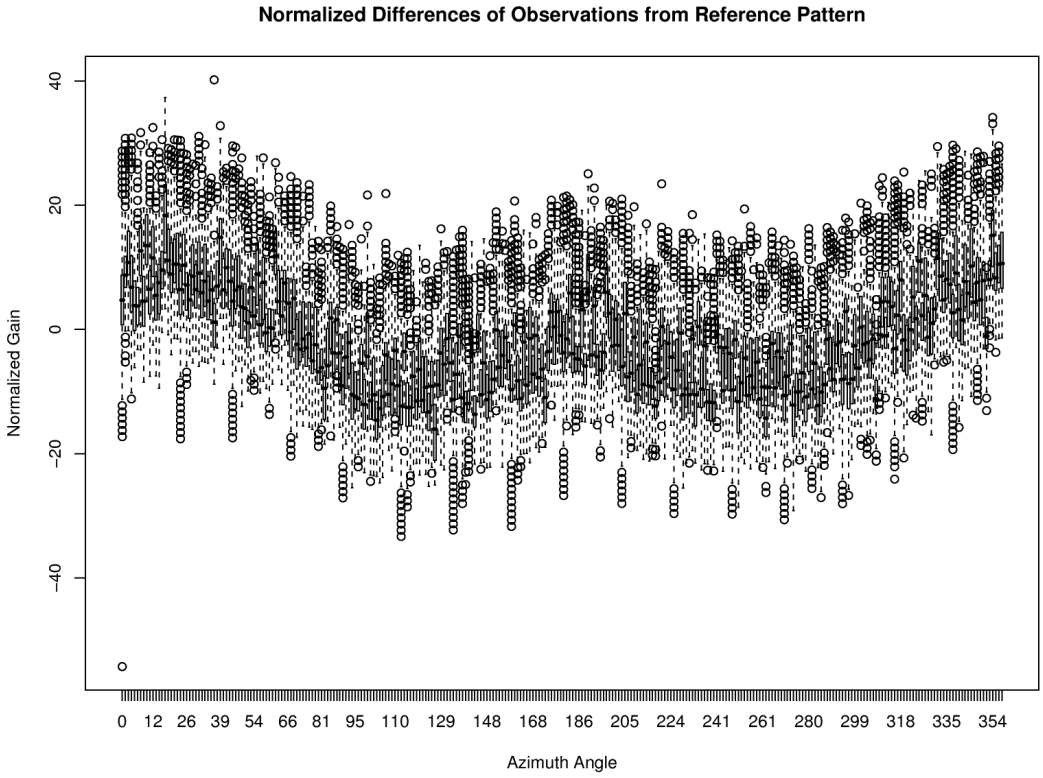


**Figure 19**: Differences between the orthogonal model and observed data in dB: $\hat{P_{rx}} - P_{rx}$: Array-Indoor-A

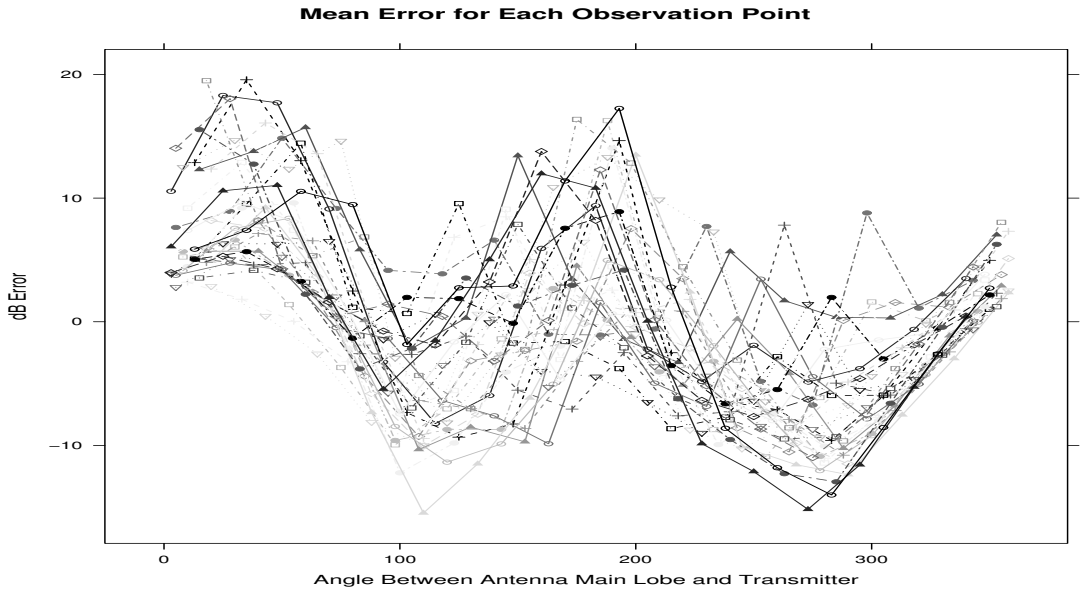


**Figure 20**: Mean error of orthogonal model for each observation point in the Array-Outdoor-A data set. The format is the same as in figures 14 through 19.

The magnitude and *systematic nature* of the error suggest that the orthogonal model has inherent limitations which cannot be alleviated by improving either the antenna model or path loss model separately.

### 5.2 An Integrated Model

This section describes a new model for the interaction of antenna direction and the RF environment. This integrated model addresses the systemic errors discussed above, while remaining simple enough to use in analysis and simulations.

We address the environment-specific, direction-specific error show in figures 14 through 20 with the following environment-aware model, given in equation 7. The expected received power is given by a constant $\beta_0$, the antenna gain function $f()$, and a yet to be determined environmental offset function $x()$:

$$\widehat{P_{rx}} = \beta_0 * f(\phi, \theta) * x(\phi, \theta) \tag{7}$$

As with the orthogonal model, we assume a constant zenith and consider $f()$ and $x()$ with regard to the azimuth $\theta$. Equation 7 can be converted to a form that lends itself to least-squares (linear regression) analysis in the following way: First, we rewrite equation 7 as addition in a logarithmic domain, and second we substitute a discrete version for the general $x()$. In the discrete $x()$, the range of angles is partitioned into $n$ bins such that bin $i$ spans the range $[B_i, T_i)$. Each bin has associated with it a boxcar function $d_i(\theta)$ to be 1 if and only if the angle $\theta$ falls within bin $i$ (equation 8) and an unknown constant *offset value* $\beta_i$. These transformations yield the model given in equation 10.

$$d_i(\theta) = \begin{cases} 1, & B_i \leq \theta < T_i \\ 0, & \text{otherwise} \end{cases} \tag{8}$$

$$x(\theta) = \sum_{i=1}^{n} d_i(\theta)\ \beta_i \tag{9}$$

$$f(\theta) - \widehat{P_{rx}} = \beta_0 + \beta_1 d_1(\theta) + \beta_2 d_2 + \cdots + \beta_n d_n(\theta) \tag{10}$$

If $x()$ is discretized into $n$ bins, the model has $n+1$ degrees of freedom: One for each bin and one for $\beta_0$, the signal strength without antenna gain. For any given signal direction, exactly one of the $d_i()$ functions will be 1, so each prediction is an interaction of two coefficients: $\beta_0$ and $\beta_i$. Consequently, $\beta_0$ could be eliminated and an equivalent model achieved by adding $b_0$'s value to each $b_i$. Mathematically, this means that there are only $n$ independent variables in the SSE fitting, and the full set is collinear. In practice, we drop the constant $b_n$, but this does not mean that packets arriving in that bin are any less well-modeled. Rather, one can think of bin $n$ as being the "default" case.

The azimuth can be divided into arbitrarily many bins. The more finely it is divided, the more degrees of freedom the model offers, and thus the more closely it can be fitted to the environment. To investigate the effect of bin number, we modeled every data set using from two to twenty bins. Figure 21 shows the residual standard error as a function of bin count. The grey box plot depicts the mean and interquartile range for all of the data collectively, and the foreground lines show values for links individually. In general, there appears to be a diminishing return as the number of bins increases, with the mean remaining nearly constant above 16 bins.

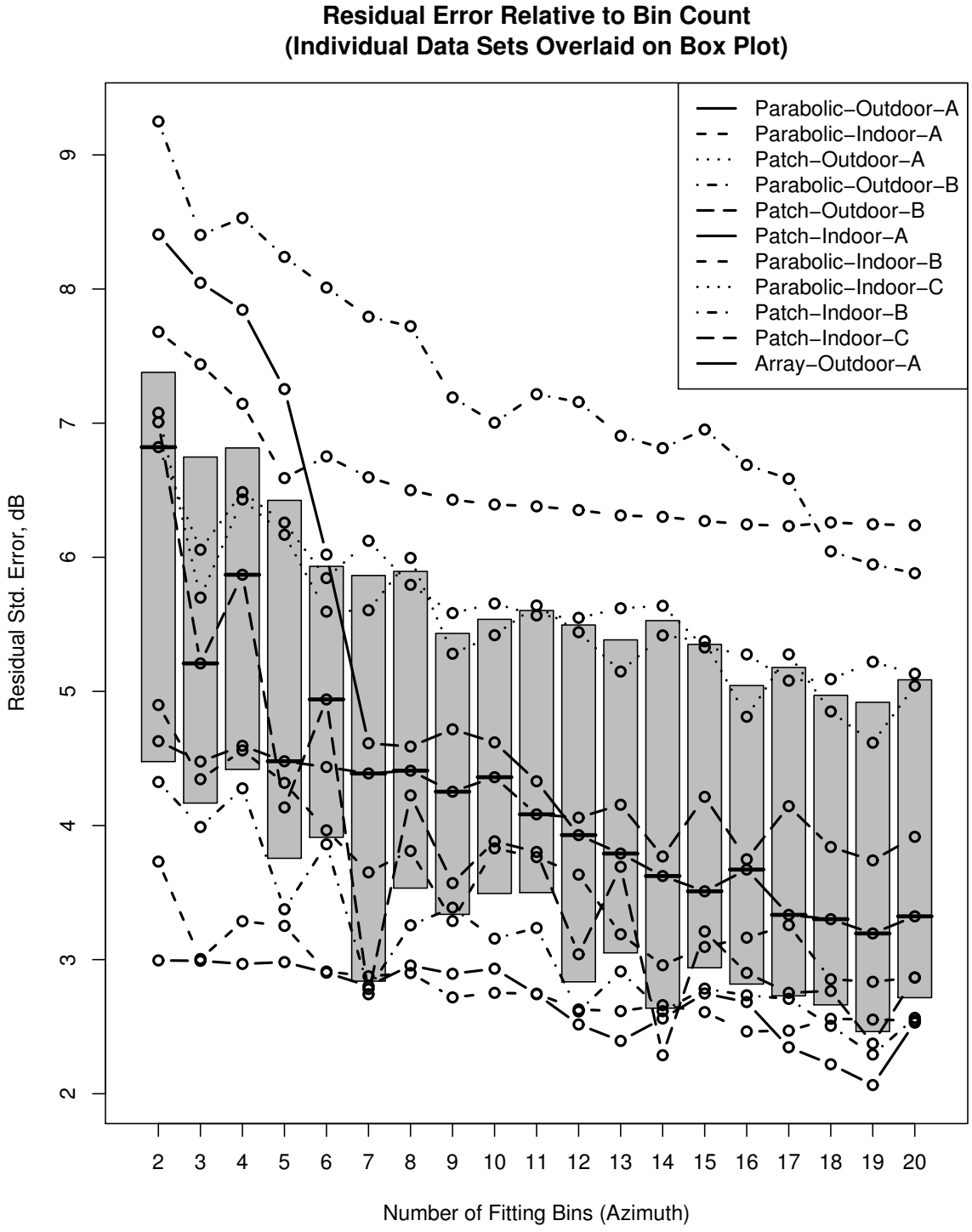


**Figure 21**: Effect of increasing bin count (decreasing bin size) on modeling precision.

In discussing parameters for this model, we will use the 16-bin case specifically. We find the same patterns across other numbers, though the actual coefficients are bin-count specific. One result of note with regard to bin count is this: Several environments exhibit a "sawtooth" pattern in which the odd bin counts do better than the even ones, or vice-versa. This appears to be an effect of the *alignment* of the bins relative to environmental features, rather than the *number* of bins as such.

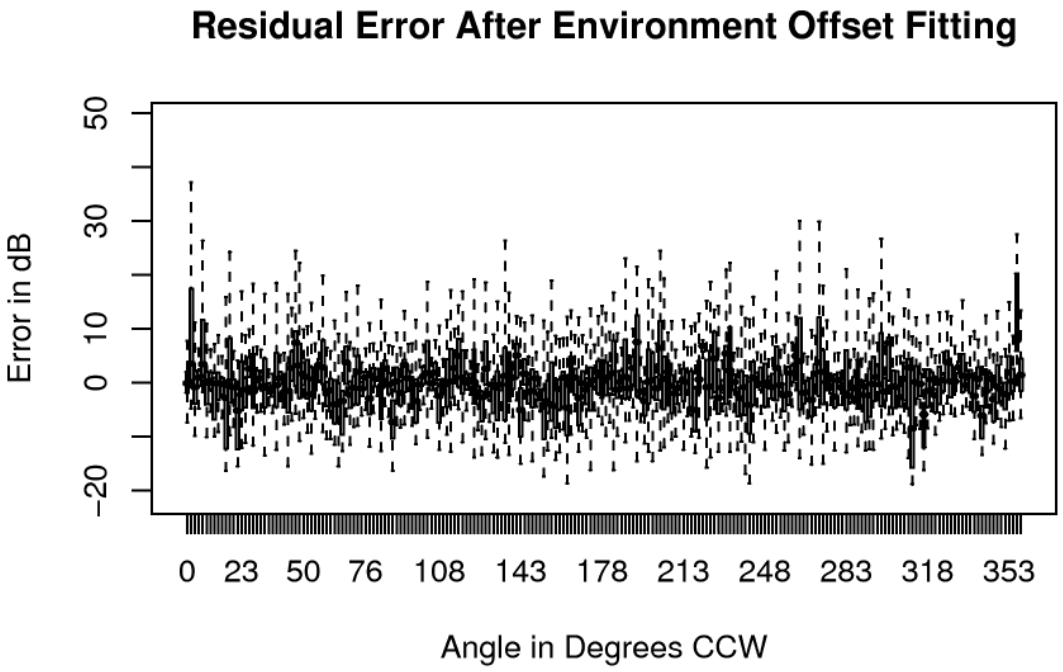


**Figure 22**: Residual error of the discrete offset model with 16 bins.

This model has significantly less error than the orthogonal model: Across all data sets, the mean residual standard error is 4.0 dB, *(4.4dB indoors)* compared to 6.15 dB *(7.312 dB indoors)* for the orthogonal model. More importantly, the error remaining in the discrete offset model is largely noise: The mean error is almost exactly zero for several ways of grouping the data. Figure 22 depicts the error (predicted value minus observed value). While the outliers reveal some direction-correlated effect that is not accounted for, this model is much better for the bulk of the traffic. Over 99.9% of the traffic *at every angle* falls within the whisker interval.

### 5.3 Describing and Predicting Environments

The environmental offset function $x()$, or its bin-offset counterpart, models the impact of a particular environment combined with a particular antenna. This can serve as an after-the-fact description of the environment encountered, but it also has predictive value: If one knows the offset function for a given environment, it is possible to more accurately model wireless systems in that environment. We are not aware of any practical way to know the exact spatial RF characteristics of an environment – and thus its offsets – without actually measuring it.

| Data Set | Factor | Coefficient | P-value |
|---|---|---|---|
| Parabolic-Outdoor-A | Antenna Gain | 0.185 | 1.02e-87 |
| | Obs. Angle | 0.00301 | 5.1e-06 |
| Patch-Outdoor-A | Antenna Gain | 0.146 | 6.4e-50 |
| | Obs. Angle | 0.00744 | 1.14e-17 |
| Array-Outdoor-A | Antenna Gain | 0.41 | 2.03e-206 |
| | Obs. Angle | -0.0271 | 5.36e-188 |
| Parabolic-Outdoor-B | Antenna Gain | 0.0377 | 8.68e-05 |
| | Obs. Angle | -0.00323 | 5.95e-05 |
| Patch-Outdoor-B | Antenna Gain | 0.00919 | 0.0492 [4] |
| | Obs. Angle | -0.00198 | 3.08e-06 |
| Parabolic-Indoor-A | Antenna Gain | 0.33 | 4.6e-102 |
| | Obs. Angle | 0.00463 | 1.91e-05 |
| Patch-Indoor-A | Antenna Gain | 0.258 | 1.22e-122 |
| | Obs. Angle | 0.00894 | 3.09e-24 |
| Parabolic-Indoor-B | Antenna Gain | 0.378 | 2.2e-134 |
| | Obs. Angle | 0.00971 | 1.97e-16 |
| Patch-Indoor-B | Antenna Gain | 0.372 | 1.1e-81 |
| | Obs. Angle | 0.014 | 3.87e-18 |
| Parabolic-Indoor-C | Antenna Gain | 0.668 | 1.39e-234 |
| | Obs. Angle | -0.0146 | 4.15e-36 |
| Patch-Indoor-C | Antenna Gain | 0.703 | 0 |
| | Obs. Angle | -0.0154 | 2.63e-48 |

**Table 2**: Factors influencing fitted offset values, 16-bin case.

However, our results suggest that it is possible to identify parameters generating the *distribution* from which the offset values for a *class of environments* are drawn.

We analyzed a range of possible determining factors for the fitted offsets, across all traces and a range of bin counts. A linear regression fit and ANOVA test found significant correlation with two factors: The nominal antenna gain $f(\theta)$ and the observation point; none of the other factors examined were consistently significant. Table 2 shows the regression coefficients and P-values for both factors for a variety of traces. The observation angle was always statistically significant, but the coefficient is constantly near zero. For each factor, the regression coefficient describes the correlation between the fitted offset and the factor. That is, the coefficient shows how much the actual signal strength can be expected to differ from the orthogonal model, for any value of that factor. For example, the antenna gain coefficients of .668 and .703 for Parabolic-Indoor-C and Patch-Indoor-C mean that in those data sets for every dB difference in antenna gain between two angles, *the-best fit difference in actual signal strength is only* $\approx$ *0.3 dB*.

There are two key results pertaining to the antenna gain regression coefficient: First, the coefficients for different antennas in the same environment are very close. Second, the coefficients for distinct but similar environments are fairly close. This suggests that classes of environments can reasonably be characterized by their associated coefficients.

[4] Marginally statistically significant.

# 6 Simulation Process

The statistical model laid out in section 5 can be used as the basis for more realistic simulations. It has long been recognized that radio propagation involves very environment-specific effects. We identify three major ways of addressing such effects in modeling and simulation: The first is to simply ignore the variability and use a single representative value in all cases. The second, which goes to the opposite extreme, is to model specific environments in great detail. A third approach is to randomly generate values according to a representative process and perform repeated experiments.

Each approach has its benefits, but we are advocating the repeated-sample approach. Precisely modeling a specific environment probably has the greatest fidelity, but it provides no information as to how well results achieved in a single environment will generalize to others. Stochastic models have the advantage of being able to produce arbitrarily many "similar" instances, and parametric models make it possible to study the impact of varying a given attribute of the environment. Such approaches are frequently used to model channel conditions [11], network topology [21, 17], and traffic load [9].

The following algorithms produce signal strength values consistent with our statistical findings. The key parameters are the gain offset correlation coefficient $K_{gain}$, the offset residual error $S_{off}$, and the per-packet signal strength residual error $S_{pss}$. We computed these values across many links for two types of environments in sections 5.3 and 5.2. Table 3 summarizes these results.

| **Environment** | $K_{gain}$ | $S_{off}$ | $S_{ss}$ |
|---|---|---|---|
| Open Outdoor | 0.01 - 0.04 | 1.326 - 2.675 | 2.68 - 3.75 |
| Urban Outdoor | 0.15 - 0.19 | 2.244 - 3.023 | 2.46 - 2.75 |
| LOS Indoor | 0.25 - 0.38 | 2.837 - 5.242 | 2.9 - 5.28 |
| NLOS Indoor | 0.67 - 0.70 | 3.17 - 3.566 | 3.67 - 6.69 |

**Table 3**: Summary of Data-Derived Simulation Parameters: Gain-offset regression coefficient ($K_{gain}$), offset residual std. error ($S_{off}$), and signal strength residual std. error ($S_{ss}$).

Algorithm 1 is a one-time initialization procedure which computes the offsets between the antenna gain in any direction and the expected actual signal gain.

Algorithm 2 computes the expected end-to-end gain for a given packet, *not including fixed path loss*. Thus, the simulated signal strength would be determined by the transmit power, path loss, receiver gain, fading model (if any), and the directional gain from algorithm 2. Note that a fading model that accounts for inter-packet variation for stationary nodes might make the random error $\epsilon$ in line 9 redundant.

# 7 Conclusion

In this paper, we have presented an empirical study of the way different environments and antennas interact to affect the directionality of signal propagation. The three primary contributions of this work are:

1. A well-validated method for surveying propagation environments with inexpensive commodity hardware.

**Algorithm 1** Compute Direction Gain

$K_{gain} \leftarrow$ gain offset correlation coefficient
$S_{off} \leftarrow$ offset residual std. error
**procedure** DIRECT-GAIN
    **for** Node $n \in$ all nodes **do**
        $P \leftarrow$ partition of azimuth range $[-\pi, \pi)$
        **for** $p_i \in P$ **do**
            $\theta_i \leftarrow$ center angle of $p_i$
            $X \leftarrow$ random value from $(\mu = 0, \sigma^2 = S_{off})$
            $o_{n,p_i} \leftarrow K_{gain} * f_n(\theta_i) + X$
        **end for**
    **end for**
**end procedure**

**Algorithm 2** Compute Per-Packet Gain

$S_{pss} \leftarrow$ residual error of packet signal strengths
**function** DIRECTIONAL-PACKET-GAIN($src, dst$)
    $\theta_{src} \leftarrow$ direction from $src$ toward $dst$
    $\theta_{dst} \leftarrow$ direction from $dst$ toward $src$
    $p_{src} \leftarrow$ partition at $src$ containing $\theta_{src}$
    $p_{dst} \leftarrow$ partition at $dst$ containing $\theta_{dst}$
    $G_{src} \leftarrow f_{src}(\theta_{src}) - o_{src,p_{src}}$
    $G_{dst} \leftarrow f_{dst}(\theta_{dst}) - o_{src,p_{dst}}$
    $\epsilon \leftarrow$ random value from $(\mu = 0, \sigma^2 = S_{pss})$
    **return**$(G_{src} + G_{dst} + \epsilon)$
**end function**

2. A characterization of several specific environments ranging from the very cluttered to the very open.

3. New, more accurate, techniques for modeling and simulating directional wireless networking.

In addition to being described in this paper, the collected data sets and simulator code implementing our model will be released to the research community.

Wireless signal – and interference – propagation is more complicated than common previous models have acknowledged. Because our models of the physical layer guide the development and evaluation of higher-layer systems, it is important that these models describe reality well enough. Our measurements, and the resulting model, bring to light several important aspects of the physical environment which previous models have failed to capture. The *effective* directionality of a system depends not only on the antenna but is influenced by the environment to such a large extent that many decisions cannot be made without in-situ measurements.

## References


[1] Crawdad. http://crawdad.org, Feb 2008.

[2] V. Abhayawardhana, I. Wassell, D. C. , M. Sellars, and M. Brown. Comparison of empirical propagation path loss models for fixed wireless access systems. In *Vehicular Technology Conference, 2005. VTC 2005-Spring. 2005 IEEE 61st*, volume 1, pages 73–77. IEEE, June 2005.

[3] J. B. Andersen, T. S. Rappaport, and S. Yoshida. Propagation measurements and models for wireless communications channels. *IEEE Communications Magazine*, 33(1):42 – 49, Jan 1995.

[4] C. R. Anderson, T. S. Rappaport, K. Bae, A. Verstak, N. Ramakrishnan, W. H. Tranter, C. A. Shadder, and L. T. Watson. In-building wideband multipath characteristics at 2.5 and 60 GHz. In *Vehicular Technlology Conference VTC*, volume 1, pages 97 – 101. IEEE, 2002.

[5] F. Babich, M. Comisso, M. D'Orlando, and L. Manià. Interference mitigation on wlans using smart antennas. *Wirel. Pers. Commun.*, 36(4):387–401, 2006.

[6] C. G. D. de Leon, M. Bean, and J. Garcia. On the generation of correlated rayleigh envelopes for representing the variant behavior of the indoor radio propagation channel. In *Personal, Indoor and Mobile Radio Communications, 2004. PIMRC 2004. 15th IEEE International Symposium on*, volume 4, pages 2757 – 2761, Sept 2004.

[7] D. green and A. Obaidat. An accurate line of sight propagation performance model for ad-hoc 802.11 wireless LAN (WLAN) devices. In *Communications, 2002. ICC 2002. IEEE International Conference on*, volume 5, pages 3424 – 3428, 2002.

[8] M. F. Iskander and Z. Yun. Propagation prediction models for wireless communication systems. *IEEE Transations on microwave theory and techniques*, 50(3):662 – 673, March 2002.

[9] I. W. Lee and A. O. Fapojuwo. Stochastic processes for computer network traffic modeling. *Computer Communications*, 29(1):1–23, December 2005.

[10] V. Navda, A. P. Subramanian, K. Dhanasekaran, A. Timm-Giel, and S. R. Das. Mobisteer: using steerable beam directional antenna for vehicular network access. In E. W. Knightly, G. Borriello, and R. Cáceres, editors, *MobiSys*, pages 192–205. ACM, 2007.

[11] A. Neskovic, N. Neskovic, and G. Paunovic. Modern approaches in modeling of mobile radio systems propagation environment. *IEEE Communications Surveys and Tutorials*, 3(3), 2000.

[12] C. Oestges and A. J. Paulraj. Propagation into buildings for broad-band wireless access. *IEEE Transactions on Vehicular Technology*, 53(2):521 – 526, March 2004.

[13] A. Plattner, N. Prediger, and W. Herzig. Indoor and outdoor propagation measurements at 5 and 60 ghz for radio lan application. In *Proc. IEEE MTT-S International Microwave Symposium Digest*, pages 853–856 vol.2, 1993.

[14] R. Ramanathan. On the performance of ad hoc networks with beamforming antennas. In *Proceedings of the 2nd ACM international symposium on Mobile ad hoc networking and computing*, pages 95–105, Long Beach, CA, USA, 2001. ACM Press.

[15] J. C. Stein. Indoor radio WLAN performance part II: Range performance in a dense office environment. Technical report, Intersil Corporation, 2401 Palm Bay, Florida.

[16] A. P. Subramanian, P. Deshpande, J. Gao, and S. R. Das. Drive-by localization of roadside wifi networks. In *27th Annual IEEE Conference on Computer Communications (INFOCOM 2008)*, Phoenix, Arizona, April 2008.

[17] H. Tangmunarunkit, R. Govindan, S. Jamin, S. Shenker, and W. Willinger. Network topology generators: degree-based vs. structural. In *SIGCOMM '02: Proceedings of the 2002 conference on Applications, technologies, architectures, and protocols for computer communications*, pages 147–159, New York, NY, USA, 2002. ACM.

[18] R. Tingley and K. Pahlavan. Space-time measurement of indoor radio propagation. *Instrumentation and Measurement, IEEE Transactions on*, 50(1):22 – 31, Feb 2001.

[19] G. Wolfle, R. Wahl, P. Wertz, P. Wildbolz, and F. Landstorfer. Deterministic propagation model for the planning of hybrid urban and indoor scenarios. In *Personal, Indoor and Mobile Radio Communications, IEEE 16th International Symposium on (PIMRC)*, volume 1, pages 659 – 663, Sept. 2005.

[20] T. A. Wysocki and H.-J. Zepernick. Characterization of the indoor radio propagation channel at 2.4 ghz. *Journal of Telecommunications and Information Technology*, 2000.

[21] E. W. Zegura, K. Calvert, and S. Bhattacharjee. How to model an internetwork. In *Infocom*. IEEE, 1996.

[22] H.-J. Zepernick and T. A. Wysocki. Multipath channel parameters for the indoor radio at 2.4 ghz ismband. In *Vehicular Technology Conference (VTC)*, volume 1, pages 190 – 193, Houston, TX, Jul 1999. IEEE.